



# Fabrication of hierarchical micro/nanostructures on titanium alloy by combining rotary ultrasonic milling and anodizing



Zhongpeng Zheng<sup>a</sup>, Jianfu Zhang<sup>a</sup>, Pingfa Feng<sup>a,b</sup>, Zhiwei Li<sup>a</sup>, Jianjian Wang<sup>a,\*</sup>

<sup>a</sup>State Key Laboratory of Tribology in Advanced Equipment, Department of Mechanical Engineering, Tsinghua University, Beijing 100084, China

<sup>b</sup>Division of Advanced Manufacturing, Shenzhen International Graduate School, Tsinghua University, Shenzhen 518055, China

## ARTICLE INFO

### Article history:

Received 10 May 2022

Received in revised form 5 July 2022

Accepted 2 September 2022

Available online 19 September 2022

### Keywords:

Hierarchical micro/nanostructures

Rotary ultrasonic milling

Anodizing

Wettability

## ABSTRACT

Hierarchical micro/nanostructures provide an efficient method for the surface wettability modulation of titanium alloy in biomedical applications. In this study, a new approach for the controllable fabrication of hierarchical micro/nanostructures is proposed by combining rotary ultrasonic milling and anodizing. Microstructures with a diameter of 90–120  $\mu\text{m}$  were fabricated by rotary ultrasonic milling, then  $\text{TiO}_2$  nanotubes with a diameter of 60–80 nm were produced on the microstructured surface by anodizing. Wettability tests demonstrate that the titanium surface with hierarchical micro/nanostructures has the lowest contact angle than that with single-level microstructures or nanostructures, verifying the efficacy of the proposed approach.

© 2022 Society of Manufacturing Engineers (SME). Published by Elsevier Ltd. All rights reserved.

## 1. Introduction

Titanium alloy is widely applied as a high-performance structural and functional material in various fields, such as aerospace, biomedicine, microfluidics, electronic devices, heat transfer, etc. Hierarchical micro/nanostructures can tune the surface properties like wettability and therefore enhance the performance of products made of titanium alloy [1]. For example, a titanium alloy surface with micro-pits and nano-nodules can enhance the proliferation and differentiation of osteoblasts in the application of orthopedic implants. Whereas the smooth implant surface cannot be firmly bonded with bone tissue, which causes the loosening of implants [2,3]. The efficient and low-cost fabrication of hierarchical micro/nanostructures plays a critical role to guarantee its large-scale industrial applications.

The fabrication methods for micro/nanostructures can be classified as mechanical and non-mechanical methods. The mechanical methods include embossing/imprinting [4], shot peening / sandblasting [5], fast/slow tool servo-assisted cutting, micro-milling, ultrasonic cutting [6,7], etc. The mechanical methods usually have high accuracy, and surface quality, but low efficiency owing to their force-based material removal/deformation principle. For example, the fast/slow tool servos-assisted cutting is capable of producing high-quality microstructures, but its production rate is low caused of the limited frequency bandwidth. The non-

mechanical methods include ion beam etching [8], laser processing [9], micro-discharge machining [10], acid etching method [11], and anodizing method. Compared with the mechanical methods, the non-mechanical method has a much smaller achievable feature size of the fabricated structures, down to several nanometers. In summary, the non-mechanical and mechanical methods have different advantages and disadvantages in efficiency, feature size, accuracy, surface quality, etc. [12] It is promising to combine mechanical and non-mechanical methods to fabricate hierarchical micro/nanostructures in two sequential steps [13–15].

Currently, there are already some applications of the combined mechanical and non-mechanical process in the fabrication of hierarchical micro/nanostructures. The most successful one is the combined process of sandblasting and acid-etching for surface treatment of dental implants made of titanium alloy. However, sandblasting has difficulties in the feature size control of microstructures, and to remove all the sand particles embedded on the material surface [16]. Recently, rotary ultrasonic milling has emerged as a superior fabrication method for surface microstructures [17–19] with much higher efficiency than other mechanical methods. In addition, rotary ultrasonic milling has process potential to texture complex free-formed surfaces of titanium alloy, which are widely applied in real-world engineering, such as the orthopedic implants [12,20]. Hence, it has great prospective to combine rotary ultrasonic milling with the non-mechanical process.

This study focuses on the feasibility evaluation of the combined process of rotary ultrasonic milling and anodizing in the

\* Corresponding author.

E-mail address: [wangjjthu@mail.tsinghua.edu.cn](mailto:wangjjthu@mail.tsinghua.edu.cn) (J. Wang).

fabrication of hierarchical micro/nanostructures on titanium alloy. The principle of the combined process is shown in Fig. 1. The microstructures are fabricated by rotary ultrasonic milling, which can flexibly control the geometries of the microstructure by multiple process parameters. Then, the nanostructures in the form of TiO<sub>2</sub> nanotubes are produced on the microstructure surface by anodizing. The wettability test of the surface with hierarchical micro/nanostructures was conducted to verify the efficacy of the combined process.

## 2. Modelling and experiments

### 2.1. Geometries control of microstructures

Since the geometries of microstructures are determined by multiple processing parameters in rotary ultrasonic milling, a simulation model of surface morphology, which can predict the effects of ultrasonic vibration amplitude, tool shape, and milling parameters is established. In special, the effects of tool edge inclination angle can be predicted by this model.

The flow chart of surface morphology simulation is shown in Fig. 2(a). In the simulation program algorithm, both space and time are discretized. The discretization of space is the discretization of the tool and the workpiece. The discretization points of the tool and the workpiece are set to discretize the space, and the time step is set to discretize the time. When the discrete points on the tool surface are lower than the discrete points on the workpiece surface, the workpiece surface will be replaced by new discrete points on the tool surface. Otherwise, the discrete points of the original artifact will be preserved. Finally, after continuous running iterations, the surface morphology of the microstructure fabricated in rotary ultrasonic milling is obtained.

The simulation model of surface morphology is based on the tool kinematic trajectory and tool contour. The tool trajectory is composed of the reciprocating vibration along the axis of the spindle and the rotational movement of the spindle. Its machining coordinate system is shown in Fig. 2(b–c). The center of the milling tool is set as the origin *O* of the coordinate system, the movement of the milling tool along the *Y*-axis is the feed movement, and the tool vibrates along the *Z*-axis. Therefore, the tool motion trajectory equation can be obtained:

$$\begin{bmatrix} x_i \\ y_i \\ z_i \end{bmatrix} = \begin{bmatrix} r \sin(2\pi n t_i / 60 + \varphi_0) \\ r \cos(2\pi n t_i / 60 + \varphi_0) + f_a t_i \\ A_L \sin(2\pi f t_i) \end{bmatrix} \quad (1)$$

where *r* is the radius of the milling tool, *n* is the rotational speed of the milling tool, *f* is the ultrasonic frequency, *f<sub>a</sub>* is the feed speed in the *y*-direction, *A<sub>L</sub>* is the amplitude of vibration, *φ<sub>0</sub>* is the initial rotation angle of the milling cutter rotation, and *t* is time.

Since the tool contour is remapped to the workpiece surface along the tool motion path, therefore, the geometric model of the tool needs to be established. Guo et al. defined a tool geometry model for the simulation of surface morphology in elliptical vibration texturing [21]. Their model doesn't consider the influence of tool edge inclination. However, there is an inclination angle *β* of the tool edge in the ultrasonic milling process, which affects the orientation of microstructures. Therefore, in this study, a general tool geometry model considering the tool edge inclination is defined as:

$$\begin{bmatrix} x_t \\ y_t \\ z_t \end{bmatrix} = \begin{bmatrix} k \cos \alpha \times \cos \beta - [(R_n - k \sin \alpha) \times \cos \psi] \times \sin \beta \\ [(R_n - k \sin \alpha) \times \cos \psi] \times \cos \beta + k \cos \alpha \times \sin \beta \\ -[R_n - k \sin \alpha] \times \sin \psi \end{bmatrix} \quad (2)$$

where *R<sub>n</sub>* is the tool edge radius, *h<sub>0</sub>* is the cutting depth considering ultrasonic vibration, *β* is the inclination angle of the tool edge, *α* is the tool clearance angle, and *ψ* is the angle between the point of the cutting edge and the *X*-axis. When *k* > 0, the parametric functions describe the flank face; when *k* < 0, the parametric functions describe the rake face, and when *k* = 0, the parametric functions describe the cutting edge.

The simulations of surface morphology of microstructure in rotary ultrasonic milling were performed under different spindle rotational speeds respectively, with results shown in Fig. 2(d–f). The tool nose radius *R* is 400 μm, the tool diameter is 10 mm, the clearance angle *α* is 10°, and the ultrasonic vibration frequency *f* is 19.5 kHz. The spacing *S* of the microstructures in the cutting direction increases as the tool rotational speed increases. The simulation results show that the profile and distribution of the microstructures can be accurately controlled by the processing parameters.

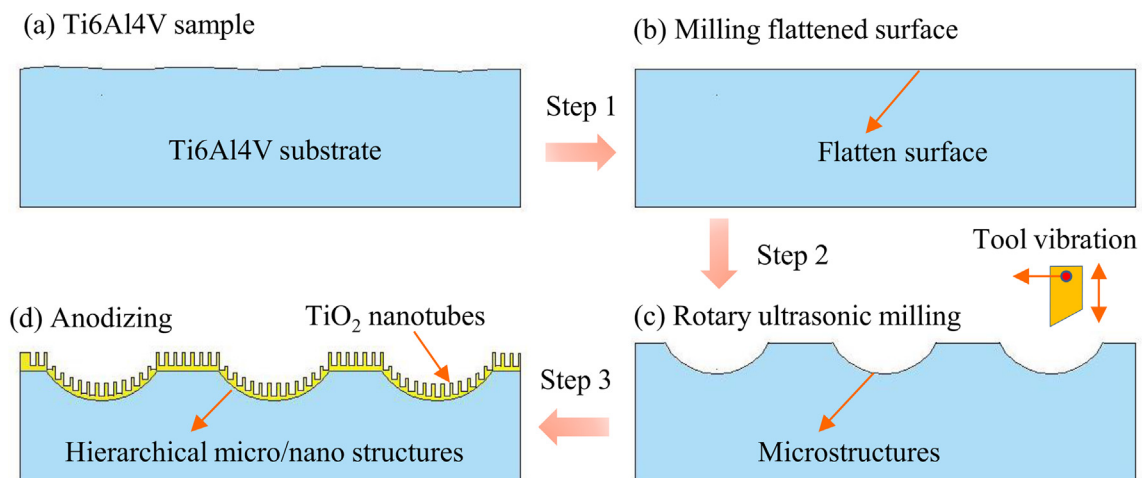


Fig. 1. Principle of hierarchical micro/nanostructure fabrication. (a) Titanium alloy sample; (b) fabrication of flattened surface; (c) fabrication of microstructures; (d) fabrication of nanostructures.

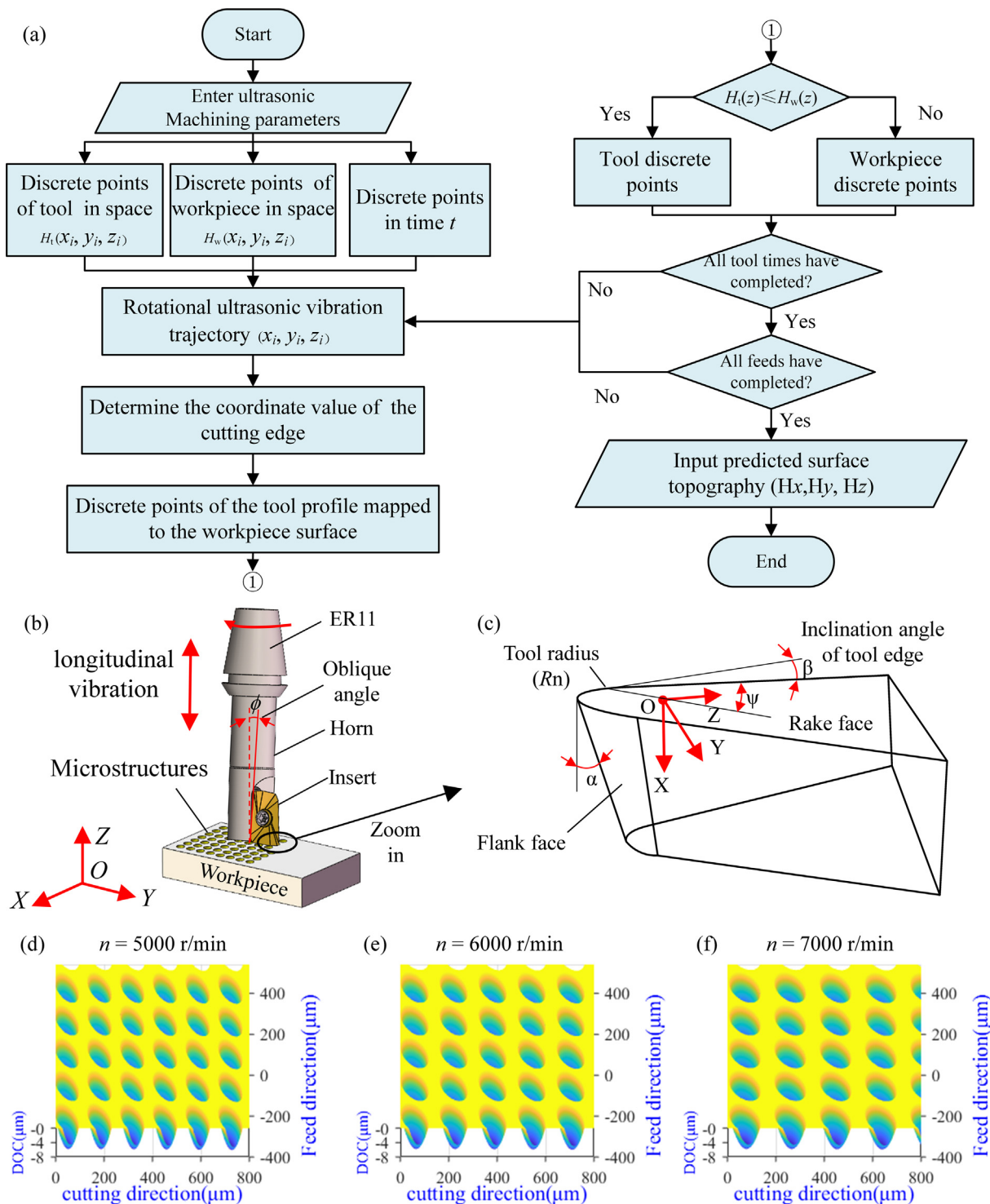


Fig. 2. (a) Flow chart of the surface morphology simulation; (b) schematic diagram of rotary ultrasonic milling; (c) cutting insert geometry definition; (d–f) simulation results.

## 2.2. Experimental design

The fabrication experiments of hierarchical micro/nanostructures by the combined rotary ultrasonic milling and anodizing process were conducted. The rotary ultrasonic milling was conducted on a 5-axis machining center (DMC Monoblock 60, Germany), which is shown in Fig. 3(b). To avoid the phenomenon of back-cutting, an oblique angle between the tool axis and the normal direction of the workpiece surface is set. The titanium alloy

Ti6Al4V was used as substrate materials. A PCD insert with a nose radius of 0.4 mm, a rake angle of  $0^\circ$ , and the clearance angle of  $10^\circ$  was used as the milling tool. In addition, a laser displacement sensor (LK-H008, Keyence Japan) with an accuracy of  $0.01 \mu\text{m}$  was used to measure the longitudinal vibration of the milling tool. The resonant frequency of the ultrasonic machining equipment was measured as 19500 Hz, which is generally consistent with the finite element analysis results. The peak-to-peak longitudinal vibration amplitude was about  $16 \mu\text{m}$ . In these experiments, the

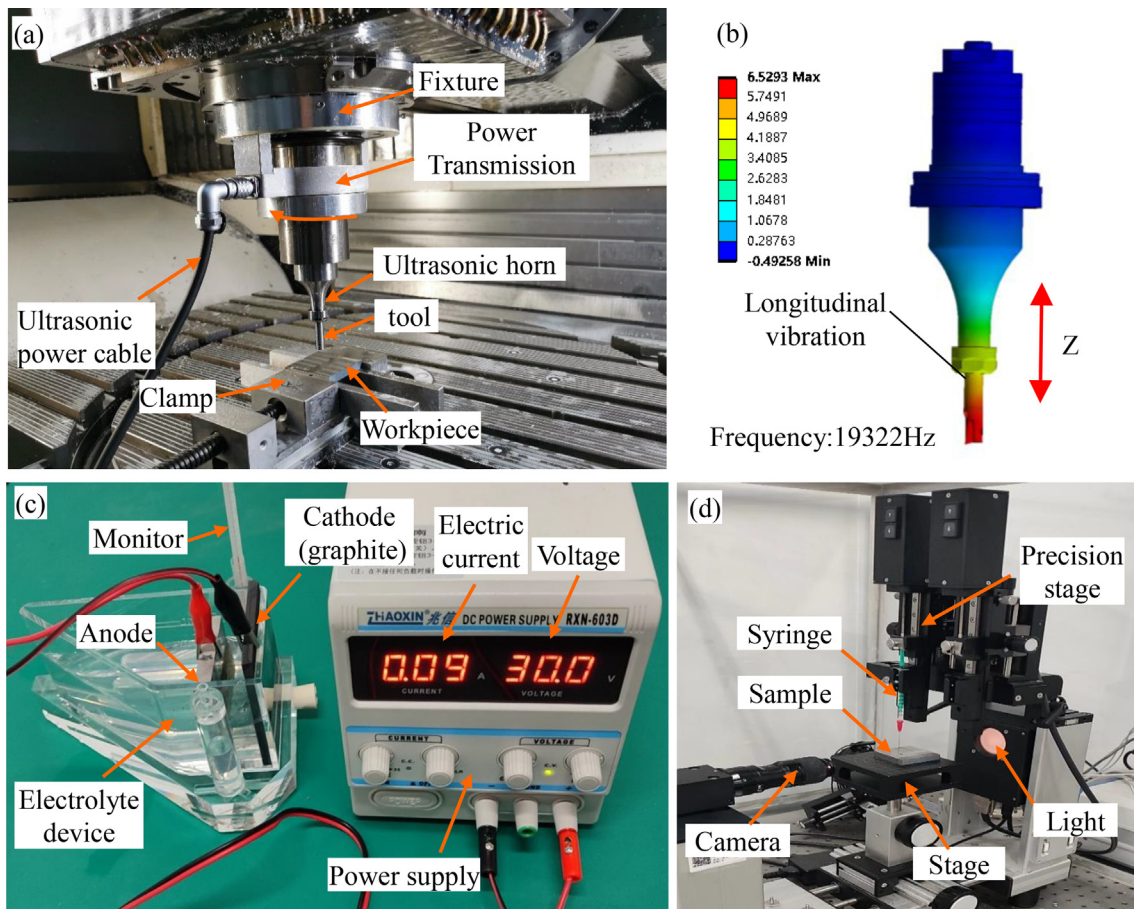


Fig. 3. Experiment setup: (a) Rotary ultrasonic milling; (b) modal analysis; (c) anodizing setup; (d) wettability setup.

workpieces were first flattened by milling using a spindle speed of 5000 rpm, a depth-of-cut of 2  $\mu\text{m}$ , and a feedrate of 0.1 mm/min. An ultrasonic frequency of 19500 Hz was used for machining microstructures with a longitudinal amplitude of 16  $\mu\text{m}$ . The surface texturing tests were conducted with spindle speeds of 5000 and 6500 rpm, a depth-of-cut of 7  $\mu\text{m}$ , feed rates of 0.12 mm/r and 0.16 mm/r, and an oblique angle of 0.15°, respectively. With these process parameters, a discrete micro dimple array can be generated.

Anodizing was conducted after rotary ultrasonic milling to produce nanostructures on the surface of microstructures. The experimental setup for anodizing is shown in Fig. 3(c). The anode is the microstructured sample, and the cathode is made of graphite material. The distance between the anode and the cathode is 10 mm, the voltage applied between the two electrodes is 30 V, and the oxidation time is 30 min. The electrolyte in the experiment contains ammonium fluoride  $\text{NH}_4\text{F}$ , deionized water, and ethylene glycol, the contents of which are 0.25 %, 2.0 %, and 97.75 %, respectively.

The surface wettability of hierarchical micro/nanostructures was compared with that of single-level microstructures or nanostructures. The surface wettability test is based on the angle formed between the tangent to the droplet surface at the three-phase boundary and the horizontal solid surface [22]. The surface contact angle (CA) was measured by using an optical static contact angle meter (Dataphysics OCA 25, Germany), which is shown in Fig. 3 (d). The suspension volume of distilled water was 3  $\mu\text{l}$ . All samples were tested at room temperature  $\sim 25^\circ\text{C}$  and humidity  $\sim 50\%$ . Each sample was measured 5 times. In addition, a confocal micro-

scope and white light interferometer were used to measure the surface profile, and a scanning electron microscope (SME) was used to observe the morphology of the hierarchical micro/nanostructures.

### 3. Results and discussion

The surface morphology of hierarchical micro/nanostructures fabricated under different processing parameters is shown in Fig. 4. Fig. 4(a–c) shows the surface morphology of the microstructures obtained by ultrasonic milling. In Fig. 4(a), the scale of microstructures is about 90–120  $\mu\text{m}$ , and the depth is about 7  $\mu\text{m}$ . The spacings between adjacent microstructures along the cutting direction and feeding direction are about 134  $\mu\text{m}$  and 160  $\mu\text{m}$  respectively, which are consistent with the theoretical results. Fig. 4(d–f) shows the surface morphology of hierarchical micro/nanostructures after anodizing. Compared with the surface with microstructures ( $S_a = 1.56 \mu\text{m}$ ), the surface with hierarchical micro/nanostructures ( $S_a = 2.4 \mu\text{m}$ ) is rougher with a roughness increase of 53 %. The SEM images of hierarchical micro/nanostructures are shown in Fig. 4(e–f). With the continuous enlargement of the surface by SEM, the  $\text{TiO}_2$  nanotubes on the surface of the titanium alloy can be observed at high magnifications. The inner diameter of the nanotubes is about 60–80 nm in diameter.

The measurement results of surface wettability are demonstrated in Fig. 4(h). The results show that the hierarchically micro/nanostructured surface has better wettability than other surfaces.

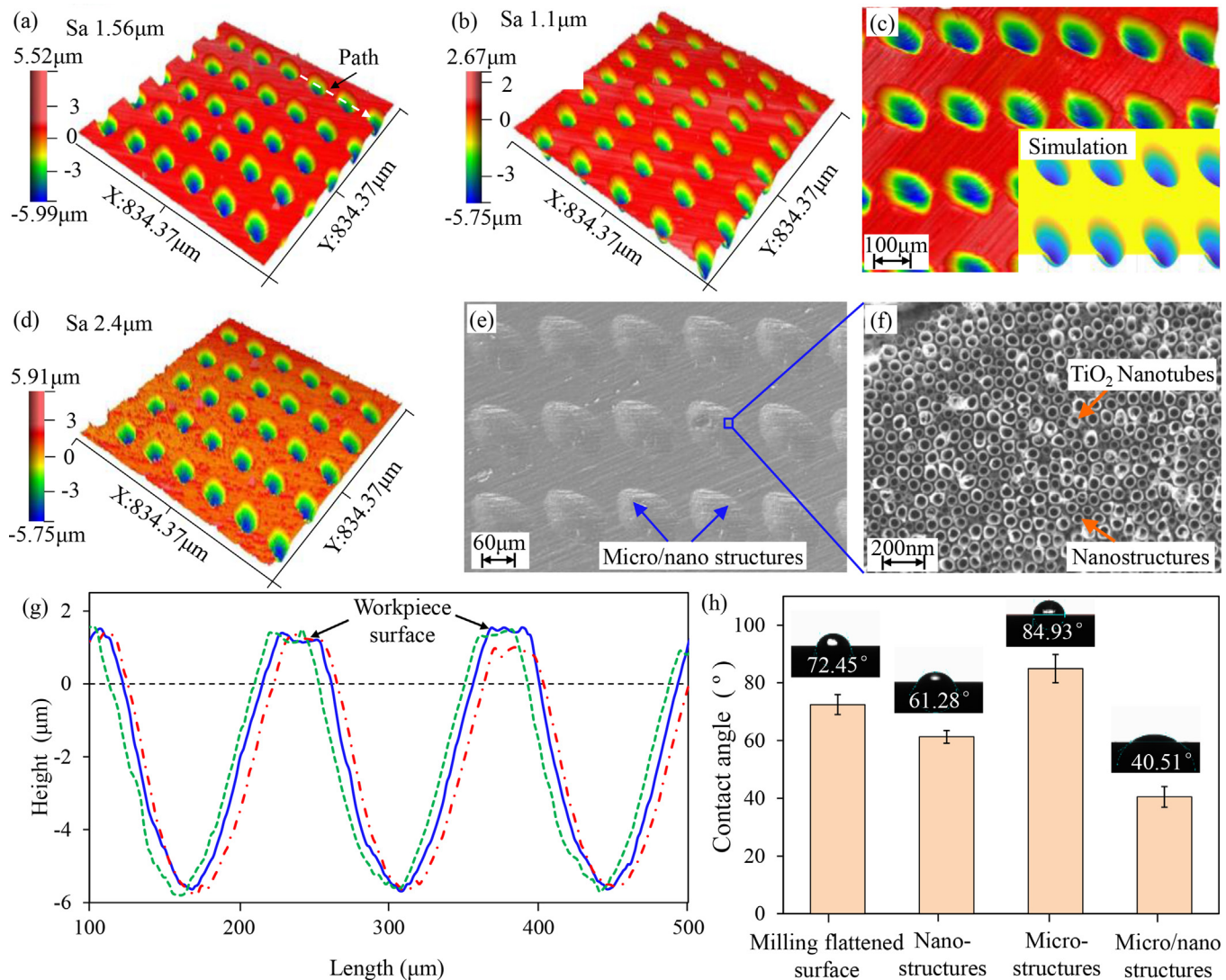


**Fig. 4.** Surface morphology and wettability of micro/nanostructures. (a & c) the micro-structures,  $n = 5000$  r/min, feed = 0.16 mm; (b) the micro-structures  $n = 6500$  r/min, feed = 0.12 mm; (d–f) the hierarchical micro/nanostructures,  $n = 5000$  r/min, feed = 0.16 mm; (g) cross-section profiles of microstructure (curves in different color denote different sampling location); (h) wettability on different surface structures,  $n = 5000$  r/min, feed = 0.16 mm.

As shown in Fig. 4(h), the contact angles of the single-level microstructured surface, nanostructured surface, and the hierarchically micro/nanostructured surface are  $84.93^\circ$ ,  $61.28^\circ$ , and  $40.51^\circ$ , respectively, while a flattened surface has a contact angle of  $72.45^\circ$ . Compared with the flattened surface, the contact angle of the microstructured surface is increased by 17.2% owing to providing more space under the water droplet and forming air pockets, thus maintaining a stable Cassie-Baxter state [23]. The contact angle of the nanostructures is reduced by 15.4%, which is mainly attributed to the siphoning effect of the capillary and the hydrophilic hydroxyl groups on the surface [11,24]. However, the contact angle of the hierarchically micro/nanostructured surface is improved by 44.08%. This excellent hydrophilicity can be attributed to the synergistic effects of microstructures and anatase  $\text{TiO}_2$  nanotubes. These experimental results verified the efficacy of the combined process in the fabrication of hierarchical micro/nanostructures on titanium alloy.

#### 4. Conclusions

This study evaluates the feasibility of the combined rotary ultrasonic milling and anodizing process for the controllable fabri-

cation of hierarchical micro/nanostructures on titanium alloy. Microstructures are firstly textured by rotary ultrasonic milling, and then nanostructures are produced on the microstructured surface by anodizing. The wettability tests of hierarchically micro/nanostructured surfaces were carried out. The main conclusions are as follows:

(1) Hierarchical micro/nanostructures were successfully fabricated on titanium alloy by combining rotary ultrasonic milling and anodizing. The feature size of the microstructures is about 90–120  $\mu\text{m}$  in diameter, 8  $\mu\text{m}$  in depth; the feature size of nanostructures in the form of  $\text{TiO}_2$  nanotubes is about 60–80 nm in diameter.

(2) A simulation model of surface morphology of microstructures fabricated by rotary ultrasonic milling was established considering the inclination angle of tool edge. This model can predict the effects of ultrasonic vibration amplitude, tool shape, and milling parameters on microstructure generation.

(3) The titanium alloy surface with hierarchical micro/nanostructures has better wettability than the flattened surface and that with single-level microstructures, and nanostructures. Compared with flattened surfaces, the contact angle of surfaces with hierarchical micro/nanostructures is improved by 44.08%.

## Declaration of Competing Interest

The authors declare that they have no known competing financial interests or personal relationships that could have appeared to influence the work reported in this paper.

## Acknowledgments

The authors gratefully acknowledge the financial support for this research provided by the National Natural Science Foundation of China (Grant No. 52105458); Tsinghua-Foshan Innovation Special Fund [No:2021THFS0204]; Huaneng Group Science and Technology Research Project (No: HNKJ22-U22YYJC08).

## References

- [1] Pratap T, Patra K. Micro-nano surface texturing, characterization, and their impact on biointerfaces. *Adv Mach Finishing*. Elsevier 2021:577–610.
- [2] Ren B, Wan Y, Liu C, et al. Improved osseointegration of 3D printed Ti-6Al-4V implant with a hierarchical micro/nano surface topography: an in vitro and in vivo study. *Mater Sci Eng, C* 2021;118:111505.
- [3] Xu Z, Huang J, He Y, Su J, Xu L, Zeng X. Fabrication of an ordered micro-/nanotextured titanium surface to improve osseointegration. *Colloids Surf, B* 2022;214:112446. <https://doi.org/10.1016/j.colsurfb.2022.112446>.
- [4] Kurita T, Ogura I, Ashida K. Proposal of laser assisted hot embossing technology for glass. *J Mater Process Technol* 2018;254:248–53.
- [5] Melentiev R, Fang F. Recent advances and challenges of abrasive jet machining. *CIRP J Manuf Sci Technol* 2018;22:1–20.
- [6] Wang J, Yang Ru, Gao S, Weng F, Wang Y, Liao W-H, et al. Modulated vibration texturing of hierarchical microchannels with controllable profiles and orientations. *CIRP J Manuf Sci Technol* 2020;30:58–67.
- [7] Wang J, Liao W-H, Guo P. Modulated ultrasonic elliptical vibration cutting for ductile-regime texturing of brittle materials with 2-D combined resonant and non-resonant vibrations. *Int J Mech Sci* 2020;170:105347. <https://doi.org/10.1016/j.iijmecsci.2019.105347>.
- [8] Golovanov AV, Bormashov VS, Luparev NV, et al. Diamond microstructuring by deep anisotropic reactive ion etching. *Physica Status Solidi (A)* 2018;215(22):1800273.
- [9] Obilor AF, Pacella M, Wilson A, Silberschmidt VV. Micro-texturing of polymer surfaces using lasers: a review. *Int J Adv Manuf Technol* 2022;120(1-2):103–35.
- [10] D'Urso G, Giardini C, Quarto M. Characterization of surfaces obtained by micro-EDM milling on steel and ceramic components. *Int J Adv Manuf Technol* 2018;97(5-8):2077–85.
- [11] Liang J, Song R, Huang Q, Yang Y, Lin L, Zhang Y, et al. Electrochemical construction of a bio-inspired micro/nano-textured structure with cell-sized microhole arrays on biomedical titanium to enhance bioactivity. *Electrochim Acta* 2015;174:1149–59.
- [12] Brinksmeier E, Karpuschewski B, Yan J, Schönemann L. Manufacturing of multiscale structured surfaces. *CIRP Ann* 2020;69(2):717–39.
- [13] Ren B, Wan Yi, Wang G, Liu Z, Huang Y, Wang H. Morphologically modified surface with hierarchical micro-/nano-structures for enhanced bioactivity of titanium implants. *J Mater Sci* 2018;53(18):12679–91.
- [14] Wang G, Wan Yi, Ren B, Liu Z. Bioactivity of micropatterned TiO<sub>2</sub> nanotubes fabricated by micro-milling and anodic oxidation. *Mater Sci Eng, C* 2019;95:114–21.
- [15] Song J, Pan W, Wang K, Chen F, Sun Y. Fabrication of micro-reentrant structures by liquid/gas interface shape-regulated electrochemical deposition. *Int J Mach Tools Manuf* 2020;159:103637. <https://doi.org/10.1016/j.ijmachtools.2020.103637>.
- [16] Nakano M, Korenaga A, Korenaga A, Miyake K, Murakami T, Ando Y, et al. Applying micro-texture to cast iron surfaces to reduce the friction coefficient under lubricated conditions. *Tribol Lett* 2007;28(2):131–7.
- [17] Wang J, Wang Y, Zhang J, et al. Structural coloration of non-metallic surfaces using ductile-regime vibration-assisted ultraprecision texturing. *Light: Adv Manuf* 2021;2(4):1–12.
- [18] Lu H, Zhu L, Yang Z, Lu H, Yan B, Hao Y, et al. Research on the generation mechanism and interference of surface texture in ultrasonic vibration assisted milling. *Int J Mech Sci* 2021;208:106681. <https://doi.org/10.1016/j.iijmecsci.2021.106681>.
- [19] Guo P, Lu Y, Pei P, Ehmann KF. Fast generation of micro-channels on cylindrical surfaces by elliptical vibration texturing. *J Manuf Sci Eng* 2014;136(4). <https://doi.org/10.1115/1.4027126>.
- [20] Pang Yu, Feng P, Wang J, Zha H, Xu J. Performance analysis of the longitudinal-torsional ultrasonic milling of Ti-6Al-4V. *Int J Adv Manuf Technol* 2021;113(5-6):1255–66.
- [21] Guo P, Ehmann KF. An analysis of the surface generation mechanics of the elliptical vibration texturing process. *Int J Mach Tools Manuf* 2013;64:85–95.
- [22] Gittens RA, Scheideler L, Rupp F, Hyzy SL, Geis-Gerstorf J, Schwartz Z, et al. A review on the wettability of dental implant surfaces ii: biological and clinical aspects. *Acta Biomater* 2014;10(7):2907–18.
- [23] Cai Y, Chang W, Luo X, Sousa AML, Lau KHA, Qin Yi. Superhydrophobic structures on 316L stainless steel surfaces machined by nanosecond pulsed laser. *Precis Eng* 2018;52:266–75.
- [24] Roy P, Dey T, Schmuki P. Scanning electron microscopy observation of nanoscopic wetting of TiO<sub>2</sub> nanotubes and ODS modified nanotubes using ionic liquids. *Electrochim Solid-State Lett* 2010;13(7):E11.